

Uncertainty Propagation in CFD Using Polynomial Chaos Decomposition

O.M. Knio ^{a,*}, O.P. Le Maître ^b

^a*Department of Mechanical Engineering, The Johns Hopkins University,
Baltimore, MD 21218, USA*

^b*Université d'Evry Val d'Essonne, CEMIF and Laboratoire d'Informatique pour la
Mécanique et les Sciences de l'Ingénieur,
LIMSI-CNRS, BP 133, F-91403 Orsay, France*

Abstract

Uncertainty quantification (UQ) in CFD computations is receiving increased interest, due in large part to the increasing complexity of physical models, and the inherent introduction of random model data. This paper focuses on recent application of Polynomial Chaos (PC) methods for uncertainty representation and propagation in CFD computations. The fundamental concept on which Polynomial Chaos (PC) representations are based is to regard uncertainty as generating a new set of dimensions, and the solution as being dependent on these dimensions. A spectral decomposition in terms of orthogonal basis functions is used, the evolution of the basis coefficients providing quantitative estimates of the effect of random model data. A general overview of PC applications in CFD is provided, focusing exclusively on applications involving the unreduced Navier-Stokes equations. Included in the present review are an exposition of the mechanics of PC decompositions, an illustration of various means of implementing these representation, a perspective on the applicability of the corresponding techniques to propagate and quantify uncertainty in Navier-Stokes computations.

Key words: Polynomial Chaos, uncertainty quantification, adaptive scheme

* Corresponding author. Tel: 1-410-516-7736; Fax: 1-410-516-7254.

Email addresses: knio@jhu.edu (O.M. Knio), olm@cemif.univ-evry.fr (O.P. Le Maître).

1 Introduction

The increasing complexity of physical models in CFD computations is frequently accompanied by the introduction of uncertain model data, such as inexact knowledge of system forcing, initial and boundary conditions, physical properties of the medium, as well as parameters in rate expressions. These situations underscore the need for efficient UQ methods, namely for the establishment of confidence intervals in computed predictions, the assessment of the suitability of model formulations, and/or the support of decision-making analysis. This paper provides a survey of recent applications of PC representations [4, 47] to propagate and quantify uncertainty in CFD computations.

PC methods rely on a probabilistic framework, which distinguishes them from alternative approaches in uncertainty assessment including fuzzy set theories, interval analysis, convex analysis, as well as linearization and perturbation methods. The fundamental concept on which PC decompositions are based is to regard uncertainty as generating a new dimension and the solution as being dependent on this dimension. A convergent expansion along the new dimension is then sought in terms of a set of orthogonal basis functions, whose coefficients can be used to quantify and characterize the uncertainty. The motivation behind PC approaches includes its suitability to models expressed in terms of partial differential equations, the ability to deal with situations exhibiting steep non-linear dependence of the solution on random model data, and the promise of obtaining efficient and accurate estimates of uncertainty. In addition, such information is provided in a format that permits it to be readily used to probe the dependence of specific observables on particular components of the input data, to design experiments in order to better calibrate or test the validity of postulated models.

Polynomial Chaos based methods have been extensively used for uncertainty quantification (UQ) in engineering problems of solid and fluid mechanics (*e.g.* elastic structures [18, 36], flow through porous media [13, 14], thermal problems [19, 24], combustion [44], and also in the analysis of turbulent velocity fields [8, 9, 38]). In contrast, application of PC methods to models involving the full (unreduced) Navier-Stokes (NS) equations is relatively more recent, though various attempts have been reported. This review focuses specifically on these applications.

Our objective is not to provide an in-depth review of the mathematical theory of PC methods, nor of its rigorous convergence proofs and accuracy estimates. Rather, we shall restrict our attention to the mechanics of the implementation of PC methods to CFD computations involving the unreduced NS equations. Section 2 provides a brief introduction to the probabilistic framework of uncertainty representation, a basic outline of PC decomposition, and then illustrates

implementation of this framework to the incompressible Navier-Stokes equations. Attention is initially focused on Galerkin approaches relying on classical Wiener-Hermite expansions [4, 47]. In section 3 a discussion is provided of computational aspects of PC operations, briefly touching on the treatment of higher-order non-linearities. Section 4 discusses alternatives to weighted residual approaches based on so-called non-intrusive formulations, while section 5 discusses generalizations of the Wiener-Hermite chaos. We conclude in section 6 with an outlook on future areas of investigation.

2 Polynomial Chaos Decompositions

The central question at hand is to characterize the solution of a problem where some of the parameters *have been* modeled as random variables or processes. PC decompositions implicitly rely on a probabilistic framework [15] in addressing this question. A random variable will thus be viewed as a function of a single variable that refers to the space of elementary events. Similarly, a stochastic process or field is then a function of $n + 1$ variables where n is the physical dimension of the space over which each realization of the process is defined.

Contrary to Monte-Carlo (MC) simulation, which can be viewed as a collocation method in the space of random variables, PC decomposition are based on coupling Hilbert space concepts –specifically projections of random functions– directly with models of computational mechanics. Random variables, defined as measurable functions from the set of basic events onto the real line, provide the mechanism for achieving such coupling, and the solution to the problem will be identified with its projection on a set of appropriately chosen basis functions. This approach is thus consistent with the identification of the space of second-order random variables* as a Hilbert space with the inner product on it defined as the mathematical expectation operation [31]. This Hilbert space structure is very convenient as it forms the foundation of many methods of deterministic numerical analysis; in addition, projections on subspaces as well as convergent approximations can now be unambiguously defined, quantified, and refined as necessary.

2.1 Random Variables and Processes

For brevity, we shall restrict our attention in this section to the case of Gaussian random variables and processes. Recall that a Gaussian process, $E(\mathbf{x}, \theta)$, can be characterized by its covariance function $R_{EE}(\mathbf{x}, \mathbf{y})$. Here, \mathbf{x} and \mathbf{y} are used to denote spatial coordinates, while θ is used to denote the random nature of the corresponding quantity. Being symmetrical and positive definite, R_{EE} has all its eigenfunctions mutually orthogonal, and they form a complete set spanning the function space to which E belongs. It can be shown that if this set of deterministic eigenfunctions is used to represent E , then the random coefficients appearing in the expansion are also orthogonal. The process can thus be expressed in terms of the well-known Karhunen-Loève (KL) expansion [31]:

$$E(\mathbf{x}, \theta) = \bar{E}(\mathbf{x}) + \sum_{i=1}^{\infty} \sqrt{\lambda_i} \xi_i(\theta) \phi_i(\mathbf{x}), \quad (1)$$

* Second-order random variables are those random variables with finite variance.

where $\bar{E}(\mathbf{x})$ is the mean of the stochastic process, $\xi_i(\theta)$ are orthogonal random variables, while $\phi_i(\mathbf{x})$ and λ_i are the eigenfunctions and eigenvalues of the covariance kernel, respectively. $\phi_i(\mathbf{x})$ and λ_i are the solution of the following integral equation:

$$\int_D R_{EE}(\mathbf{x}, \mathbf{y}) \phi_i(\mathbf{y}) d\mathbf{y} = \lambda_i \phi_i(\mathbf{x}), \quad (2)$$

where D denotes the domain over which $E(\mathbf{x}, \theta)$ is defined.

Note that the KL expansion is mean-square convergent irrespective of the probabilistic structure of the process being expanded, provided it has finite variance [31]. The closer a process is to white noise, the more terms are required in the expansion. Conversely, a Gaussian random variable, α , be represented by a single term, i.e. the KL expansion can be reduced to:

$$\alpha = \bar{\alpha} + \sigma_\alpha \xi \quad (3)$$

where $\bar{\alpha}$ is the mean, σ_α is the standard deviation, and ξ is normalized Gaussian with unit standard deviation.

2.2 Polynomial Chaos Decomposition

The covariance function of the solution process is not known *a priori*, and hence the KL expansion may not be used to approximate it. Furthermore, even when the problem specification only involves Gaussian parameters or processes, the solution process is not necessarily Gaussian, so that the KL representation may not be a suitable approximation even when much is known about the covariance function of the solution. Thus, an alternative representation means is needed, and the PC decomposition addresses this need.

Since the solution process, u , is a function of the random data, it is natural to seek to represent it as a non-linear functional of the ξ_i 's that are used to represent the random data. It can be shown [4] that this functional dependence can be expressed in terms of polynomial functions of the ξ_i , known as polynomial chaoses, according to:

$$u = a_0 \Gamma_0 + \sum_{i_1=1}^{\infty} a_{i_1} \Gamma_1(\xi_{i_1}) + \sum_{i_1=1}^{\infty} \sum_{i_2=1}^{\infty} a_{i_1 i_2} \Gamma_2(\xi_{i_1}, \xi_{i_2}) + \dots \quad (4)$$

where $\Gamma_n(\xi_{i_1}, \dots, \xi_{i_n})$ denotes the Polynomial Chaos [20, 47] of order n in the variables $(\xi_{i_1}, \dots, \xi_{i_n})$. The polynomial chaoses are usually generalized multidimensional Hermite polynomials of independent variables that are measurable

functions with respect to the Wiener measure. In particular, when the independent variables are identified as the Gaussian vector $\boldsymbol{\xi} = (\xi_1, \xi_2, \dots, \xi_n)$, one recovers the familiar expression of the expectation:

$$\langle f \rangle = \frac{1}{(2\pi)^{n/2}} \int_{-\infty}^{\infty} f(\boldsymbol{\xi}) \exp\left(-\frac{|\boldsymbol{\xi}|^2}{2}\right) d\boldsymbol{\xi} \quad (5)$$

where $|\boldsymbol{\xi}|^2 = \sum_{i=1}^n \xi_i^2$.

The zero, first, and second-order polynomials are given by [18]:

$$\Gamma_0 = 1, \quad \Gamma_1(|x_i|) = \xi_i, \quad \Gamma_2(\xi_i, \xi_j) = \xi_i \xi_j \delta_{ij} \quad (6)$$

where δ_{ij} is the Kronecker delta. For computational purposes, the “generic” PC representation (4) must be suitably truncated, and this is typically performed by retaining polynomials of order $\leq p$, where p is a prescribed value. It is also convenient (section 3) to introduce a one-to-one mapping between the set of indices appearing in the truncated sum corresponding to (4) and a set of ordered indices, and rewrite the truncated sum in (4) in single-index form according to:

$$u \simeq \sum_{j=0}^P u_j \Psi_j \quad (7)$$

where the Ψ_j denote the polynomial chaoses in single-index notation, while $P+1$ is the total number of polynomials chaoses of order $\leq p$. Note that for the one-dimensional case, $P = p$, while in a space with n stochastic dimensions [11]

$$P = \frac{(p+n)!}{p!n!} - 1. \quad (8)$$

Note that the polynomials are mutually orthogonal, in the sense that the inner product $\langle \Psi_i \Psi_j \rangle = 0$ when $i \neq j$. Moreover, the set $\{\Psi_j\}_{j=1}^{\infty}$ can be shown to form a complete basis in the space of second-order random variables. Specifically, any second-order process u has a mean-square convergent expansion given in equation (4) where $\Gamma_p(\cdot)$ is the Polynomial Chaos of order p [4]. Also note that the PC expansion can be used to represent, in addition to the solution process, both Gaussian and non-Gaussian model data. One can verify this by observing that the first summation in an expansion of the form given by Eq. (4) represents a Gaussian component; thus, for a Gaussian function, expansion (4) reduces to a single summation, the coefficients a_{i_1} being the coefficients in the Karhunen-Loève expansion of the function [12, 18]. Accordingly,

the additional summations in the expansion are immediately identified as representing the non-Gaussian behavior of the function in terms of a non-linear, (polynomial) functional dependence on the independent Gaussian variables.

In order to obtain a complete probabilistic characterization of the solution process, u , it is sufficient to determine the “deterministic” coefficients u_j appearing in Eq. (7). Due to the orthogonality of the Ψ 's, the coefficients of the PC expansion of u satisfy:

$$u_j = \frac{\langle u \Psi_j \rangle}{\langle \Psi_j^2 \rangle}, \quad (9)$$

for $j = 0, \dots, P$. As mentioned in the introduction, we shall primarily focus on determination of the u_j 's using a Galerkin approach, and the latter is initially outlined for a generic stochastic process, u , governed by:

$$\mathcal{O}(u(\boldsymbol{\xi}), \boldsymbol{\xi}) = 0, \quad (10)$$

where \mathcal{O} is a non-linear operator. The Galerkin scheme is based on introducing the expansion (7) into (10) and taking orthogonal projections onto the truncated basis, which results in the following system for the basis function coefficients:

$$\left\langle \mathcal{O} \left(\sum_i u_i \Psi_i(\boldsymbol{\xi}), \boldsymbol{\xi} \right), \Psi_j \right\rangle = 0, \quad j = 0, \dots, P. \quad (11)$$

Solution of the above coupled system then yields the desired coefficients. Below, we focus on implementation of this approach to the incompressible NS equations.

2.3 Application to the Incompressible NS Equations

Application of the PC decomposition above is illustrated by outlining the construction of the stochastic projection method (SPM) as originally introduced in [25]. The SPM focuses on the numerical solution of the incompressible NS equations:

$$\frac{\partial \mathbf{u}}{\partial t} + (\mathbf{u} \cdot \nabla) \mathbf{u} = -\nabla p + \nu \nabla^2 \mathbf{u} \quad (12)$$

$$\nabla \cdot \mathbf{u} = 0 \quad (13)$$

where $\mathbf{u} = (u, v)$ is the velocity vector, t is time, p is the pressure, and ν the kinematic viscosity. For brevity, we focus on the solution of Eqs. (12-13) in a 2D domain, D , with specified velocity boundary conditions on ∂D satisfying:

$$\int_{\Gamma} \mathbf{u}_n dA = 0 \quad (14)$$

where $\Gamma = \partial D$ is the boundary of D , \mathbf{u}_n is the component of \mathbf{u} normal to Γ , and dA is the surface element along Γ . We also restrict our attention to the case of a single parameter, and illustrate the case of a Gaussian initial condition:

$$\mathbf{u}(\mathbf{x}, t = 0) = \bar{\mathbf{u}}(\mathbf{x}) + \xi \mathbf{u}'(\mathbf{x}) \quad (15)$$

where ξ is a Gaussian variable with unit variance, and $\bar{\mathbf{u}}(\mathbf{x})$ and $\mathbf{u}'(\mathbf{x})$ are given quantities. Note that in the present case $\bar{\mathbf{u}}$ and \mathbf{u}' represent the mean and standard deviation of the initial velocity field, respectively. One can immediately verify this claim from the definitions of mean and variance applied to each of the velocity components. For instance, for the u component, we have:

$$\langle u(\mathbf{x}, t = 0) \rangle \equiv \langle \bar{u}(\mathbf{x}) + \xi u'(\mathbf{x}) \rangle = \bar{u}(\mathbf{x}), \quad \text{and} \quad (16)$$

$$\sigma_{u(\mathbf{x}, t=0)} \equiv \left\langle (u(\mathbf{x}, t = 0) - \langle u(\mathbf{x}, t = 0) \rangle)^2 \right\rangle^{1/2} = |u'(\mathbf{x})|. \quad (17)$$

The development of the SPM is based on inserting the PC decompositions of all stochastic quantities into the NS equations, and applying the Galerkin procedure to derive governing equations for the individual modes appearing in these expansions. This results in a system of the form:

$$\frac{\partial \mathbf{u}_k}{\partial t} + \sum_{i=0}^P \sum_{j=0}^P \mathcal{M}_{ijk} (\mathbf{u} \cdot \nabla) \mathbf{u} = -\nabla p_k + \nu \nabla^2 \mathbf{u}_k \quad (18)$$

$$\nabla \cdot \mathbf{u}_k = 0 \quad (19)$$

for $k = 0, \dots, P$. Note that the quadratic term involves a convolution sum involving the multiplication tensor:

$$\mathcal{M}_{ijk} \equiv \frac{\langle \Psi_i \Psi_j \Psi_k \rangle}{\langle \Psi_k^2 \rangle} \quad (20)$$

Boundary and initial conditions are also decomposed in a similar fashion. In particular, for the latter we have: $\mathbf{u}_0(\mathbf{x}, t = 0) = \bar{\mathbf{u}}(\mathbf{x})$, $\mathbf{u}_1(\mathbf{x}, t = 0) = \mathbf{u}'(\mathbf{x})$, and $\mathbf{u}_k(\mathbf{x}, t = 0) = 0$ for $k = 2, \dots, P$.

SPM relies a fractional step projection scheme in order to integrate the evolution equations of the stochastic modes. In a first fractional step, we integrate the coupled advection-diffusion equations:

$$\frac{\partial \mathbf{u}_k}{\partial t} + \sum_{i=0}^P \sum_{j=0}^P \mathcal{M}_{ijk}(\mathbf{u}_i \cdot \nabla) \mathbf{u}_j = \nu \nabla^2 \mathbf{u}_k \quad (21)$$

for $k = 0, \dots, P$. An explicit multi-step scheme may be used for this purpose. For instance, for a second-order Adams-Bashforth scheme we have:

$$\frac{\mathbf{u}_k^* - \mathbf{u}_k^n}{\Delta t} = \frac{3}{2} \mathbf{H}_k^n - \frac{1}{2} \mathbf{H}_k^{n-1} \quad k = 0, \dots, P \quad (22)$$

where \mathbf{u}_k^* are the predicted velocity modes, Δt is the time step,

$$\mathbf{H}_k \equiv \nu \nabla^2 \mathbf{u}_k - \sum_{i=0}^P \sum_{j=0}^P \mathcal{M}_{ijk}(\mathbf{u}_i \cdot \nabla) \mathbf{u}_j, \quad (23)$$

and the superscripts refer to the time level. In the second fractional step, a pressure correction is performed in order to satisfy the divergence constraints on the velocity modes. We have:

$$\frac{\mathbf{u}_k^{n+1} - \mathbf{u}_k^*}{\Delta t} = -\nabla p_k \quad k = 0, \dots, P \quad (24)$$

where the pressure fields p_k are determined so that the fields \mathbf{u}_k^{n+1} satisfy the divergence constraints in (19), i.e.

$$\nabla \cdot \mathbf{u}_k^{n+1} = 0 \quad (25)$$

Combining equations (24) and (25) results in the following system of *decoupled* Poisson equations:

$$\nabla^2 p_k = -\frac{1}{\Delta t} \nabla \cdot \mathbf{u}_k^* \quad k = 0, \dots, P \quad (26)$$

Similar to the original projection method [7], the above Poisson equations are solved, independently, subject to Neumann conditions that are obtained by projecting equation (24) in the direction normal to the domain boundary [7, 22].

Remarks

- (1) One of the key advantages of SPM is that the numerical formulation effectively exploits the fact that the velocity divergence constraints are *decoupled*, which results in a set of $P + 1$ decoupled pressure projection steps. Since these steps typically account for the bulk of the computational effort in incompressible flow simulations, the solution of the stochastic system can be at essentially a cost of $P + 1$ deterministic solutions. Coupled with the spectral nature of the stochastic representation, this leads to a highly efficient stochastic solver, as illustrated in Fig. 1 below.

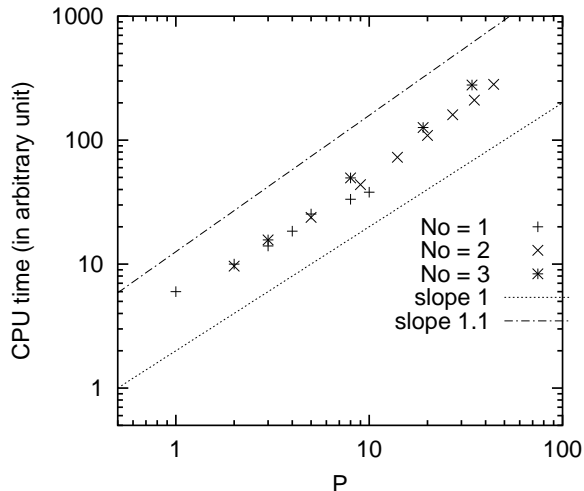


Fig. 1. Dependence of the CPU time on the number of modes P in SPM computations of internal, gravity-driven flow under stochastic temperature boundary conditions. The spatial discretization is on a staggered, finite-difference grid, with conservative second-order differences. Results with first, second, and third-order PC expansions are reported, respectively $p = N_o = 1, 2,$ and 3 . Adapted from [29].

- (2) By relying an integral formulation, the Galerkin stochastic approach outlined above is well suited for essentially any numerical discretization scheme. Specifically, the approach has been used extensively in conjunction with finite element methods [12,16–18]; NS computations using spectral element methods [49] have also been reported, as well as upwind finite-difference schemes [34]. Thus, the latter experiences indicate that the Galerkin PC formulation naturally overcomes some of the limitations of linearized or perturbation approaches, which typically face severe difficulties with non-smooth filtering operations used in upwind schemes.

2.4 Other Navier-Stokes Implementations

PC-based UQ schemes have been applied in simulations of more elaborate NS formulations, simulations of microfluid systems [10], nearly incompressible

Boussinesq flows [29], weakly compressible flow at low-Mach-number [28], reacting flow [39], as well as fully compressible unsteady flow in a single space dimension [33].

For brevity, we focus our attention on Galerkin approaches following the development outlined in section 2.2, and to multi-dimensional momentum solvers. Thus, we shall omit from the present discussion 1D compressible flow computations [33], and reacting flow models [39]. Also omitted are stochastic simulations of microfluidic systems [10], as the latter incorporate essentially the same incompressible momentum update as in SPM [25, 29].

An immediate, though non-trivial, generalization of the incompressible SPM concerns weakly-compressible Boussinesq flows. This situation was considered in [29], which focused on simulation of a stochastic variant of the coupled system:

$$\frac{\partial \mathbf{u}}{\partial t} + \mathbf{u} \cdot \nabla \mathbf{u} = -\nabla p + \frac{\text{Pr}}{\sqrt{\text{Ra}}} \nabla^2 \mathbf{u} + \text{Pr} \theta \mathbf{y}, \quad (27)$$

$$\nabla \cdot \mathbf{u} = 0, \quad (28)$$

$$\frac{\partial \theta}{\partial t} + \nabla \cdot (\mathbf{u} \theta) = \frac{1}{\sqrt{\text{Ra}}} \nabla^2 \theta. \quad (29)$$

where θ is the normalized temperature, while Pr and Ra denote the Prandtl and Rayleigh numbers, respectively. Generalization of the SPM outlined above to the case of Boussinesq flow is deemed immediate, since the major modifications involve incorporation of the buoyancy source term in the momentum equation, and the simultaneous integration of an advection equation for temperature. The structure of the pressure projection steps, on the other hand, remains unchanged, as the presence buoyancy source terms only affects their right-hand-sides. Thus, at least in the case of SPM, generalization from incompressible to Boussinesq flow requires a straightforward adaptation of the stochastic scheme.

In contrast, generalization of stochastic incompressible NS solver to compressible zero-Mach-number flows can prove significantly more challenging. Such an exercise was considered in [28], which focused on extension of SPM to simulation of natural convection in a heated cavity under non-Boussinesq conditions. The simulations were based on a stochastic variant on the compressible NS equations in the zero-Mach-number limit [6, 32]:

$$\frac{\partial \rho}{\partial t} = -\nabla \cdot \rho \mathbf{u} \quad (30)$$

$$\frac{\partial(\rho u)}{\partial t} = -\frac{\partial(\rho u^2)}{\partial x} - \frac{\partial(\rho uv)}{\partial y} - \frac{\partial \Pi}{\partial x} + \frac{1}{\sqrt{\text{Ra}}} \Phi_x \quad (31)$$

$$\frac{\partial(\rho v)}{\partial t} = -\frac{\partial(\rho uv)}{\partial x} - \frac{\partial(\rho v^2)}{\partial y} - \frac{\partial \Pi}{\partial y} + \frac{1}{\sqrt{\text{Ra}}} \Phi_y - \frac{1}{\text{Pr}} \frac{\rho - 1}{2\epsilon} \quad (32)$$

$$\frac{\partial T}{\partial t} = -\mathbf{u} \cdot \nabla T + \frac{1}{\rho \text{Pr} \sqrt{\text{Ra}}} \nabla \cdot (\kappa \nabla T) + \frac{\gamma - 1}{\rho \gamma} \frac{d\bar{P}}{dt} \quad (33)$$

$$\bar{P} = \rho T \quad (34)$$

where ρ is the density, Π is the hydrodynamic pressure, Ra is the Rayleigh number, ϵ is the temperature (Boussinesq) ratio, Φ_x and Φ_y are the viscous stress terms in the x and y directions, respectively, Pr is the Prandtl number, κ is the normalized thermal conductivity, γ is the specific heat ratio, and $\bar{P}(t)$ is the thermodynamic pressure [45].

As explained in [28], one delicate aspect of the generalization of SPM to zero-Mach-number flows concerns enforcement of the mass conservation constraints. In the numerical scheme constructed in [28], these constraints lead to the following decoupled system of elliptic equations for the hydrodynamic pressure modes:

$$\nabla^2 \Pi_k = \frac{1}{\Delta t} \left[\nabla \cdot (\rho \mathbf{u})_k^* + \frac{\partial \rho_k}{\partial t} \right]^{n+1}, \quad k = 0, \dots, P \quad (35)$$

with homogeneous Neumann boundary conditions. These equations are thus subject to the following solvability constraints:

$$\int_{\Omega} \frac{1}{\Delta t} \left[\nabla \cdot (\rho \mathbf{u})_k^* + \frac{\partial \rho_k}{\partial t} \right]^{n+1} d\Omega = 0 \quad (36)$$

In many situations, particularly in the case of a conservative discretization, the integral of the divergence term in Eq. (36) may be given as an integral over known boundary terms, and may thus be evaluated exactly. In particular, in the case of a domain bounded by stationary solid boundaries, the integral of the divergence term vanishes identically. On the other hand, the integral of the second term is significantly more delicate, because the density evolution equation involves complex combinations of stochastic quantities which, generally, can only be approximately estimated. Consequently, without special care, the solvability constraints may only be approximately satisfied. As experienced in [28], this situation always led to unstable computations. To overcome this difficulty, a special procedure for the evaluation of the global mass conservation constraint was developed in [28]. The procedure ensured that solvability constraints were satisfied to machine precision, which resulted in a stable solver.

Note that in the case of a constant density flow, the time derivative in Eq. (36)

vanishes identically, while the integral of the divergence term also vanishes due to the global mass (volume) conservation constraint (Eq. 14). Thus, unlike the case of zero-Mach-number flow, for a conservative discretization the solvability conditions of the Poisson equations for the stochastic pressure modes are immediately satisfied. Consequently, extensions of incompressible solvers to zero-Mach-number flows should include a suitable treatment of the mass divergence constraints.

3 PC computations

In this section we review some key concepts for the manipulation and implementation of stochastic spectral expansions.

3.1 Quadratic products

In their simplest unreduced form, the unreduced NS equations involve quadratic (convective) non-linear terms. Consequently, the determination of the spectral expansion of the quadratic product of the form $c = ab$, where a and b are given by:

$$a(\boldsymbol{\xi}) = \sum_{i=0}^P a_i \Psi_i(\boldsymbol{\xi}) \text{ and } b(\boldsymbol{\xi}) = \sum_{j=0}^P b_j \Psi_j(\boldsymbol{\xi}), \quad (37)$$

is of primary interest. Applying the definition of the projection on the spectral basis, we obtain the expression for the spectral coefficients of c , namely:

$$c_k \langle \Psi_k^2 \rangle \equiv \langle c \Psi_k \rangle = \langle (ab) \Psi_k \rangle = \sum_{i=0}^P \sum_{j=0}^P a_i b_j \langle \Psi_i \Psi_j \Psi_k \rangle. \quad (38)$$

Introducing the multiplication tensor \mathcal{M}_{ijk} defined in Eq. (20), Eq. (38) can be rewritten as:

$$c_k = \sum_{i=0}^P \sum_{j=0}^P \mathcal{M}_{ijk} a_i b_j. \quad (39)$$

The above convolution sum is a true Galerkin projection of c onto the subspace spanned by the Ψ_k , $k = 0, \dots, P$, but that higher-order terms, namely those involving polynomials of order $> p$ are, of course, ignored. It is also interesting to note that, formally, Eq. (39) suggests that the operation count needed to determine a quadratic product is essentially $O(P^3)$. However, due to the sparse nature of \mathcal{M} , the operation count is actually much smaller. As further discussed in section 3.4, taking advantage of the ‘‘sparseness’’ of \mathcal{M} is key for computational efficiency.

One can exploit Eq. (39) to derive expression for the PC expansion of the inverse of a stochastic quantity. Letting b denote the inverse of a , we have by definition:

$$(ab)_k = \sum_i \sum_j \mathcal{M}_{ijk} a_i b_j = \delta_{0k} \quad (40)$$

where δ denote the Kronecker delta. Since the coefficients a_i are known, the above expression can be recast as a system of $(P + 1)$ linear equations in the unknown coefficients b_k , $k = 0, \dots, P$. A standard linear equation solver can then be used to solve the system and hence determine the PC expansion of b .

3.2 Higher-order transformations

For many fluid problems of interest, the formulation involves complex physical models requiring higher-order transformations of spectral quantities. A well-known example concerns reacting flows, where the governing equations include quadratic products as well as complex source terms involving higher-order products, exponentiation, inversion, etc. . . These complex functionals require suitable spectral estimates, which, generally, may only constitute approximate Galerkin projections; balancing precision and computation cost is, in these situations, an important consideration.

3.2.1 Higher-order products

Consider first the ternary product $d = abc$. One can apply the same Galerkin procedure used for quadratic products, which in the present case gives:

$$d_l = \sum_{i=0}^P \sum_{j=0}^P \sum_{k=0}^P \mathcal{T}_{ijkl} a_i b_j c_k \quad (41)$$

where

$$\mathcal{T}_{ijkl} \equiv \frac{\langle \Psi_i \Psi_j \Psi_k \Psi_l \rangle}{\langle \Psi_l \Psi_l \rangle}. \quad (42)$$

Although \mathcal{T} is also sparse, it has a significantly larger number of non-zero entries than \mathcal{M} , and Galerkin evaluation of d requires substantially higher storage and CPU cost than a quadratic product. In order to reduce these requirements, an alternative “pseudo-spectral” evaluation approach can be implemented, based on successive application of the formula for quadratic products. For instance, d may be estimated using:

$$d_k \approx \sum_i \sum_j (ab)_i c_j \mathcal{M}_{ijk}, \text{ where } (ab)_i = \sum_m \sum_n a_m b_n \mathcal{M}_{mni}. \quad (43)$$

The drawback of this approximate factorization is that it may introduce aliasing errors. We also note that in general

$$\sum_i \sum_j (ab)_i c_j \mathcal{M}_{ijk} \neq \sum_i \sum_j (ac)_i b_j \mathcal{M}_{ijk} \neq \sum_i \sum_j (bc)_i a_j \mathcal{M}_{ijk}, \quad (44)$$

and so using the pseudo-spectral approach the spectral representation of d depends on the order in which the approximate factorization is applied. However, if the expansion order p is large enough, one may expect the resulting errors to be small, as observed in actual computations. Also note that the same factorization procedure can be applied to higher-order terms, writing for instance $abcd = [(ab)c]d$.

3.2.2 Taylor series approach

Let $f(a)$ denote a function of a stochastic quantity a with known PC representation. The Taylor expansion of $f(a)$ about the mean of $a = a_0$ is

$$f(a) = f(a_0) + \sum_{l=1}^{\infty} \frac{(a - a_0)^l}{l!} f^{(l)}(a_0),$$

where $f^{(l)} = d^l f / da^l$. If f is well behaved and the variance of a sufficiently small, one can expect the Taylor series to converge quickly with l . In this case, the series can be truncated after the first few terms, requiring only the estimation of the first powers of $\tilde{a} \equiv a - a_0 = \sum_{i=1}^P a_i \Psi_i$, using for instance the pseudo-spectral approach outlined above. However, if the Taylor series converges slowly, the computation of the PC expansion of \tilde{a}^l , from $\tilde{a}^{l-1}a$, may be plagued by significant errors as l increases, thus restricting the domain of application for the Taylor series approach.

3.2.3 Simulation approach

A robust means for overcoming the limitation of the Taylor series approach consists of avoiding approximation of higher powers, instead relying on sampling or simulation to directly determine the PC representation of $f(a)$. Since the spectral coefficients f_i of $f(a)$ are by definition given by $\langle f(a) \Psi_i \rangle / \langle \Psi_i^2 \rangle$, one can apply the following sampling procedure to determine f_i :

$$\langle f \Psi_i \rangle \approx \sum_{s=1}^{N_s} f(a(\boldsymbol{\xi}_s)) \Psi_i(\boldsymbol{\xi}_s) w(\boldsymbol{\xi}_s), \quad (45)$$

where N_s is the number of samples, and $(\boldsymbol{\xi}_s, w_s)$ are the sample points and associated weights. Different sampling strategies can be used, including non-

deterministic sampling (e.g. Monte-Carlo, Latin hypercube, ...), quadrature, and cubature formulas (see section 4). It is emphasized that this approach only requires the computation of f for different (deterministic) values of its random argument $a(\boldsymbol{\xi})$. The principal limitation of this simulation strategy concerns the number of sample points Ns needed to achieve sufficient accuracy. Specifically, the computational cost may be prohibitively large in situations where a large value of Ns is needed to ensure small sampling errors.

3.3 Integration approach

This approach, recently introduced in [11], is based on differentiation of f , followed by integration along a prescribed path. In the deterministic case, and provided that f can be differentiated, $f(a)$ can be computed through the integration of its derivative $g(a) = df/da$:

$$f(a) - f(\tilde{a}) = \int_{\tilde{a}}^a g da,$$

where \tilde{a} is an arbitrary starting point where f can be evaluated. This idea can be extended to the stochastic case as follow. First, consider the random processes:

$$\begin{aligned} b &= b(s, \boldsymbol{\xi}) = \sum_{i=0}^P b_i(s) \Psi_i(\boldsymbol{\xi}), \\ f &= f(s, \boldsymbol{\xi}) = \sum_{i=0}^P f_i(s) \Psi_i(\boldsymbol{\xi}), \\ g &= g(s, \boldsymbol{\xi}) = \sum_{i=0}^P g_i(s) \Psi_i(\boldsymbol{\xi}), \end{aligned}$$

where s parametrized the integration path across the deterministic space of PC coefficients, and g is still the derivative of f . The random process $b(s, \boldsymbol{\xi})$ is arbitrary selected such that it evolves along the integration path from $b = \tilde{b}(\boldsymbol{\xi})$ where $f(\tilde{b})$ can be easily evaluated, to $b = a(\boldsymbol{\xi})$ at the end of the integration.

Assuming that b , f and g are analytic with respect to s , we have

$$\int_{s_1}^{s_2} \frac{\partial f}{\partial s} ds = \int_{s_1}^{s_2} g \frac{\partial b}{\partial s} ds, \quad (46)$$

and the result of the integration being path-independent. Equation (46) may

be rewritten as:

$$\sum_{i=0}^P \Psi_i \int_{s_1}^{s_2} \frac{df_i}{ds} ds = \sum_{i=0}^P [f_i(s_2) - f_i(s_1)] \Psi_i = \sum_{i=0}^P \sum_{j=0}^P \Psi_i \Psi_j \int_{s_1}^{s_2} g_i(s) \frac{db_j}{ds} ds. \quad (47)$$

Projecting onto the PC basis, we obtain for each index k :

$$f_k(s_2) = f_k(s_1) + \sum_i \sum_j \int_{s_1}^{s_2} \mathcal{M}_{ijk} g_i(s) \frac{db_j}{ds} ds. \quad (48)$$

Then, given an integration path such that $f(b(s_1, \boldsymbol{\xi}))$ can be easily evaluated, and $b(s_2, \boldsymbol{\xi}) = a(\boldsymbol{\xi})$, we obtain

$$f_k(s_2) = \frac{\langle f(a) \Psi_k \rangle}{\langle \Psi_k^2 \rangle} = f_k(s_1) + \sum_i \sum_j \int_{s_1}^{s_2} \mathcal{M}_{ijk} g_i \frac{db_j}{ds} ds. \quad (49)$$

In practice, the integration path from s_1 to s_2 is defined as:

$$\begin{cases} b_0(s) = a_0, \\ b_k(s) = a_k \frac{s - s_1}{s_2 - s_1} \quad k > 0, \end{cases} \quad (50)$$

such that $f_k(s_1) = f(a_0)$ for $k = 0$ and 0 for $k > 0$, and $f_k(s_2) = f_k(a)$. Then, the integration can be performed using standard techniques as long as the spectral expansion of g , the derivative of f , can be computed along the integration path.

Though the approach appears to have merely shifted the difficulty in evaluating the PC expansion of f to that of its derivative, it still enables us to resolve a wide class of non-linear transformations, such as exponentials, logarithms and powers of a [11]). Compared with the Taylor series approach, this integration technique is more costly, due to multiple evaluations of the PC expansions of g along the integration path. However, numerical tests have shown its effectiveness for situations with large variance of the argument, where application of the Taylor series approach is limited.

3.4 Computational strategies

An efficient implementation of PC expansions is a crucial step in conversion of a deterministic code into a stochastic PC-based counterpart. In this section,

we provide here details on the so-called UQ-toolkit, which comprises a library of utilities that help streamline deterministic code conversions.

3.4.1 PC constructs

One of the key features in PC implementation concerns the tensor construction of the multi-dimensional basis functions. For brevity, we illustrate these constructs using the classical Hermite-based PC expansions.

The multi-dimensional Hermite polynomials are constructed from tensor products of the one-dimensional Hermite polynomials. Let $H_i(\xi)$ denote the 1-D Hermite polynomial of order $i > 0$ in ξ . Then the corresponding $\Psi_i(\boldsymbol{\xi})$ is given by:

$$\Psi_i(\boldsymbol{\xi}) = \prod_{j=1}^n H_{\alpha_j^{(i)}}(\xi_j), \quad (51)$$

where $\alpha^{(i)} \equiv \{\alpha_1^{(i)}, \dots, \alpha_n^{(i)}\}$ is the multi-index of the polynomial Ψ_i . The order of Ψ_i is $p_i = \sum_{j=1}^n \alpha_j^{(i)}$. By convention, $\alpha^{(0)} = \{0, \dots, 0\}$, so that $\Psi_0(\boldsymbol{\xi}) = 1$, while the multi-indices for the first order polynomials are given by:

$$\alpha^{(i)} = \{0, \dots, 0, \alpha_i^{(i)} = 1, 0, \dots\} \quad \text{for } i = 1, \dots, n, \quad (52)$$

yielding $\Psi_{i=1, \dots, n} = \xi_i$. Polynomials with order $1 < p_i \leq p$ are typically determined by systematically “looping” over the various dimensions [23], and this results in an ordered the representation of the Ψ_i 's and the corresponding multi-indices. The ordering scheme is in fact a key underlying feature of all PC operations.

3.4.2 Construction of the multiplication tensor

Determination of the multiplication tensor involves the evaluation of the expectation of triple products of the form $\Psi_i \Psi_j \Psi_k$. Using the multi-index definition, we have:

$$\begin{aligned} \langle \Psi_i \Psi_j \Psi_k \rangle &= \left\langle \left(\prod_{m=1}^n H_{\alpha_m^{(i)}}(\xi_m) \right) \left(\prod_{m=1}^n H_{\alpha_m^{(j)}}(\xi_m) \right) \left(\prod_{m=1}^n H_{\alpha_m^{(k)}}(\xi_m) \right) \right\rangle \\ &= \prod_{m=1}^n \langle H_{\alpha_m^{(i)}} H_{\alpha_m^{(j)}} H_{\alpha_m^{(k)}} \rangle, \end{aligned} \quad (53)$$

where we have made use of the statistical independence of the ξ 's. Equation (53) shows that the multidimensional multiplication tensor can be de-

terminated based on knowledge of the one-dimensional expectations $\langle H_i H_j H_k \rangle$. The latter can be established using symbolic computations or tables (see for instance [18]), or alternatively using the Gauss-Hermite quadratures [1, 23]. Equation (53) also reveals the origin of the sparseness of \mathcal{M} , as it is sufficient that the 1-D expectation vanishes along one stochastic dimension to have $\mathcal{M}_{ijk} = 0$.

Taking advantage of the multi-index construction, only the non-zero entries of the multiplication tensor are computed during a pre-processing stage, and stored using a sparse format for subsequent use in the computations.

3.5 UQ toolkit

Extension of a deterministic code to incorporate the PC representation of uncertainty consists of two elementary steps. First, all quantities and fields that depend on the uncertainty are extended to involve a supplementary index that corresponds to the single-index representation of the PC basis. The ordering scheme determined in the multi-index construct is also used for the present purpose. For instance, in a two-dimensional problem the deterministic discrete velocity \mathbf{u}_{ij} , defined at the node (i, j) of a spatial mesh, is extended to \mathbf{u}_{ijk} where the two first indices still refer to the spatial location, while k refers to the polynomial index. In other words, the uncertain velocity at node (i, j) has for expansion:

$$\mathbf{u}_{ij}(\theta) = \sum_k \mathbf{u}_{ijk} \Psi_k(\boldsymbol{\xi}(\theta)). \quad (54)$$

After this index extension is implemented for all relevant variables, it is necessary to re-interpret all operations involving these quantities. Some of these operations are not affected by the uncertainty, as spatial differentiation for instance, and need only to be repeated for all modes $0 \leq k \leq P$. On the other hand, require a spectral treatment as discussed in this section 3.1. As an example, consider the computation of the convective terms $u\partial u/\partial x$ arising in the momentum equation. In a first stage, we compute the spatial derivatives $\partial u_i/\partial x = (\partial_x u)_i$ for all modes. Then, in a second stage, the spectral coefficients of the convective term, $(u\partial_x u)_k$, are determined by applying the multiplication rule in (39), resulting in:

$$(u\partial_x u)_k = \sum_i \sum_j \mathcal{M}_{ijk} u_i (\partial_x u)_j. \quad (55)$$

Note that the operations above involve local grid information, and so can be easily and efficiently parallelized. Moreover, since the multiplication tensor is

sparse and stored in sparse format, it is advantageous to systematically rely on a subroutine that takes advantage of this feature. For instance in Fortran-like language, the spectral coefficients of the convective terms of our example would be obtained through

```
call prod(u,dudx,ududx)
```

where `u` and `ududx` are two arrays of length $P + 1$ containing the spectral coefficients of u and $\partial_x u$ respectively, and `prod` returns the coefficients of their product in the array `ududx`. In a similar way, higher-order operations are also implemented through systematic calls to subroutines contained in the UQ toolkit.

4 Non-intrusive formulations

In this section, we discuss an alternative to spectral computations which consists of performing the projection of the stochastic flow solution onto the spectral basis using a set of *deterministic* solutions. Since this approach does not require solution of the governing equations for the spectral modes, but needs only the availability of a deterministic solver, it is termed “non-intrusive,” the terminology emphasizing the fact that modification of the deterministic solver is neither required nor performed. By construction, the non-intrusive approach can also be qualified as a collocation method, as opposed to Galerkin method, since the projection is performed based on specific realizations or points in the random parameter space. The non-intrusive alternative is especially attractive in situations where one wants to propagate and quantify uncertainties in a complex problem using a deterministic code that should not be modified, for instance using commercial, legacy or certified codes. Another interesting feature of the non-intrusive approach is that it naturally circumvents the difficulties associated with the spectral treatment of high-order non-linearities.

As in the Galerkin method, the starting point of uncertainty quantification and propagation in the non-intrusive context is the parametrization of the input-uncertainties. Again, we assume that the input random data are parametrized using a set of n independent and normalized Gaussian variables $\boldsymbol{\xi}(\theta) = \{\xi_1(\theta), \dots, \xi_n(\theta)\}$, and are interested, in particular, in the determination of the velocity modes \mathbf{u}_k , $k = 0, \dots, P$. The orthogonality of the spectral basis provides the following expressions for \mathbf{u}_k ,

$$\langle \Psi_k^2 \rangle \mathbf{u}_k = \langle \mathbf{u}(\boldsymbol{\xi}(\theta)) \Psi_k(\boldsymbol{\xi}(\theta)) \rangle = \int \mathbf{u}(\boldsymbol{\xi}) \Psi_k(\boldsymbol{\xi}) \text{pdf}(\boldsymbol{\xi}) d\boldsymbol{\xi}, \quad (56)$$

where, using the independence of the ξ_i 's,

$$\text{pdf}(\boldsymbol{\xi}) = \prod_{i=1}^n \frac{\exp[-\xi_i^2/2]}{\sqrt{2\pi}}. \quad (57)$$

Equation (56) shows that the velocity modes can be determined through the computation of the integrals on its right-hand side. Different means can be used to estimate these integrals, leading to the methods outlined below.

4.1 Stochastic methods

The first class of methods discussed here is based on stochastic sampling strategies. The simplest of these methods is the Monte-Carlo (MC) approach (see

e.g. [30]), which relies on an unbiased sampling of the random parameter space. In unbiased MC, The integrals are computed using:

$$\int \mathbf{u}(\boldsymbol{\xi}) \Psi_k(\boldsymbol{\xi}) \text{pdf}(\boldsymbol{\xi}) d\boldsymbol{\xi} = \lim_{N_{mc} \rightarrow \infty} \frac{1}{N_{mc}} \sum_{m=1}^{N_{mc}} \mathbf{u}(\boldsymbol{\eta}_m) \Psi_k(\boldsymbol{\eta}_m), \quad (58)$$

where the $\boldsymbol{\eta}_m$ are pseudo-random vectors, with independent components, generated following the distribution of $\boldsymbol{\xi}$ given in Eq. (57). The flow has to be solved for each realization of the uncertain parameters, as prescribed by $\boldsymbol{\eta}_m$. It is known that the convergence rate for unbiased sampling is $1/\sqrt{N_{mc}}$ in the asymptotic limit $N_{mc} \rightarrow \infty$, so the precision of the MC projection method is inherently limited for large problems where the computation of individual realizations are expensive. More complex (biased) stochastic sampling techniques can be used to improve the convergence rate. There is a vast literature on improvement of MC sampling strategies, including variance reduction techniques, stratified sampling, Latin-Hypercube sampling, and most of these techniques are readily applicable to the integral in Eq. (56). In [29], we performed a non-intrusive numerical experiment for a natural convection flow inside a closed cavity, involving $n = 6$ uncertain parameters, and using a Latin-Hypercube sampler (LHS) [37]. The comparison with the Galerkin computation for the same flow, clearly put in evidence the much lower efficiency of the LHS non-intrusive approach both in terms of CPU cost and accuracy. Note, however, that for problems with large number, n , of stochastic dimensions, the Galerkin approach may face limitations due to memory requirements, while in contrast the computation of individual realizations is insensitive to the number of stochastic dimensions involved in the underlying uncertainty sources. The main limitation of non-intrusive methods appears to be due to the number of realizations needed to properly sample the parameter space. Note also that different realizations of the flow are independent and can be computed on parallel; for example, in [29] a 64-processor machine was used to take advantage of this feature.

4.2 Deterministic methods

In problems with a moderate number of stochastic dimensions, it may be advantageous to apply a deterministic approach to compute the integrals in Eq. (56), since deterministic methods usually exhibit greater flexibility in rate of convergence and accuracy control. This section discusses two possible deterministic methods.

4.2.1 Gauss-type quadratures

For $n = 1$, Eq. (56) can be written as:

$$\langle \Psi_k^2 \rangle \mathbf{u}_k = \int_{-\infty}^{+\infty} \mathbf{u}(\xi) \Psi_k(\xi) \frac{\exp(-\xi^2/2)}{\sqrt{2\pi}} d\xi. \quad (59)$$

Using the Gauss-Hermite (GH) quadrature formula [1], the integral can be estimated using the finite sum:

$$\langle \Psi_k^2 \rangle \mathbf{u}_k \approx \sum_{i=1}^{N_q} \mathbf{u}(x_i) \Psi_k(x_i) w_i, \quad (60)$$

where the (x_i, w_i) , $i = 1, \dots, N_q$, are the Gauss-Hermite quadrature points and weights. This formula is exact for polynomial integrands with degree $\leq 2N_q - 1$. The 1D formula can be easily extended to multidimensional situations ($n > 1$) through a straightforward tensor product extension. This strategy was used in [29] to perform a deterministic non-intrusive projection for the same flow problem mentioned above ($n = 6$). For this test case, it provided velocity modes that are in excellent agreement (same level of accuracy) with the Galerkin computations. In terms of CPU cost, the GH method was more expensive than the Galerkin solution. Specifically, when the Galerkin computation is optimized such that the corresponding CPU cost scales essentially as P -times the CPU cost of a deterministic solution, where P is the dimension of the stochastic basis, it is possible to obtain a simple estimate of the relative cost between Galerkin and non-intrusive GH methods. Fig. (2) provides this estimate for different values of n and p . The plot shows that the GH approach becomes impractical for high dimensional problems, because of the number of realizations that scales as N_q^n . This ‘‘curse’’ of dimensionality is a well known limitation of quadrature formulas, and different ‘‘sparse’’ alternatives designed to maintain precision for high dimensional integration have been proposed in the literature. In the following section, we discuss one of these approaches, which has been applied in the context of UQ in [21, 35].

It is interesting to note that Gauss-type quadratures are also available (e.g. see [1]) for most classical basis functions used in generalized PC decompositions (section 5). Thus, the applicability of Gauss-type quadratures extends beyond the classical Wiener-Hermite chaos.

4.2.2 Sparse cubature

The curse of dimension of the tensor Gauss-type quadrature formulas can be circumvented using coarser quadratures, which can still provide exact esti-

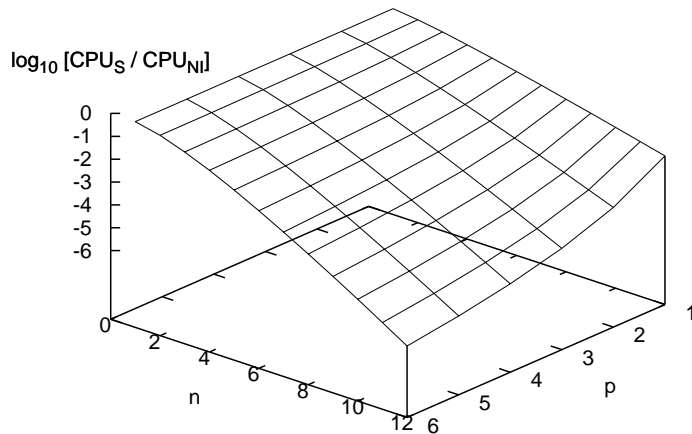


Fig. 2. Evolution with the number of stochastic dimensions n and expansion order p , of the ratio of CPU_S , the CPU cost of the Galerkin computation (assuming a linear scaling with the basis dimension $P + 1$) with CPU_{NI} the CPU cost of non-intrusive projection using the tensor Gauss-Hermite formula.

mates in the same subspaces as the multi-dimensional Gauss-type quadrature [40–42]. These coarse formulas, known as cubature rules, are based on algorithmic constructions such as the Smolyak scheme [43,46], and result in a number of cubature points that could challenge the efficiency of the Galerkin computations for large n . As an example, we provide in Fig. (3) the number of cubature points necessary for an exact integration of polynomial functions of order N_o , for an increasing number of dimensions $N_d = n$. To our knowledge, such cubature formulas have not been tested yet for the propagation of uncertainties in fluid flows governed by the Navier-Stokes equations. However, some experiments have been successfully performed in the context of ground-water flows governed by elliptic stochastic equations [21,35], and one would in fact expect that a similar success in applications to NS problems.

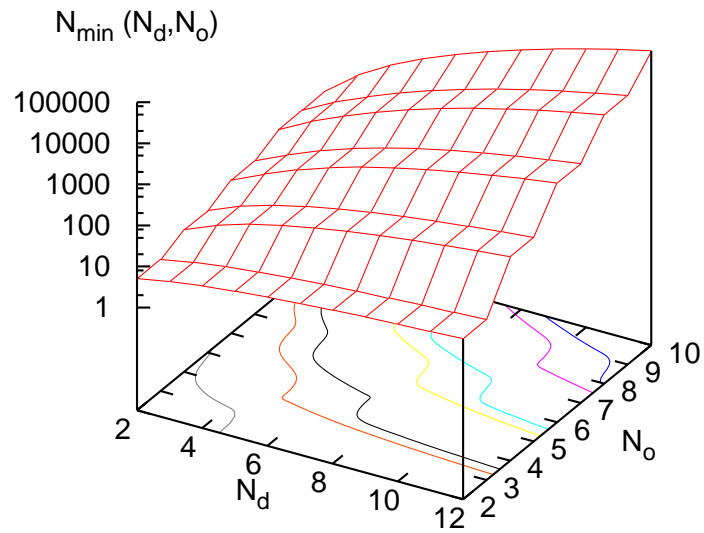


Fig. 3. Example of the evolution of the number cubature points N_{\min} needed to achieve exact integration for polynomial integrands of degree N_o , and different number of stochastic dimensions $N_d = n$, using the Smolyak construction scheme. This evolution has to be compared with the Gauss-type tensor formula where N_{\min} scales with $(N_o + 1)^n / 2^n$.

5 Generalized PC

Classical PC representations are based on a well-established theoretical foundation that takes advantage of the fact that the Hermite chaos is complete and orthogonal with respect to the Wiener measure [4]. In particular, Wiener-Hermite expansions are well suited when representing random data corresponding to Gaussian variables and processes.

Note, however, that it is possible to apply alternative orthogonal basis functions in PC expansions. This section outlines possible alternatives, and briefly addresses the question concerning their suitability and whether specific advantages may be derived from their implementation. The discussion focuses exclusively on chaos decompositions corresponding to continuous measures, and considers separately the cases of local and global basis functions.

5.1 Global Basis Functions

A general construction that captures several possible choices of PC representations is the so-called Wiener-Askey family, originally developed by Askey and Wilson [3] and first introduced in the UQ context by Xiu and Karniadakis [48]. In addition to the Hermite chaos, the Wiener-Askey family in particular includes Laguerre and Jacobi basis functions. The latter are orthogonal polynomials in random variables that follow gamma and beta distributions, respectively, orthogonality being naturally interpreted with respect to the corresponding measures.

From an implementation perspective, the computational framework of the UQ toolkit outlined above enables the user to navigate freely between different basis representations. Most of the effort associated with a change of basis concerns the construction of the multiplication tensor(s), and procedures for other nonlinear transformations in case they are not based directly on the latter. Thus, this effort is limited to pre- and post-processing, with little or no change to the structure of the stochastic code. This is another key feature of the UQ toolkit.

It is also interesting to note, much like the Hermite case, PC representations based on the Laguerre and Jacobi polynomials are expected to exhibit exponential convergence as the order of the corresponding expansion is increased. Such convergence behavior is in fact guaranteed whenever certain smoothness conditions are satisfied [5]. In such situations, selection of a specific basis function representation would primarily be based on convenience, and to a lesser extent on the “efficiency” of the presentation –since the latter is *generally* not known *a priori*.

In their original development [48], Xiu and Karniadakis provided several examples in which the input random data have pdf's that correspond to those of the random variables of basis functions belonging to Wiener-Askey chaos. They show through computational examples that it can be more advantageous to select a basis representation whose random variables have a similar distribution as the input random data. This is especially the case when the distribution of the input data are such that exponential convergence is immediately lost when other basis function representations are selected.

One should note, however, that a rapidly convergent spectral representation of the input random data may not always constitute a key consideration in the selection of a basis function representation. To support this assertion, one observes that PC representation generally provides a complete functional representation of the response of the stochastic solution in terms of the random variables. Specifically, one can readily determine particular solutions corresponding to specific realizations of the random variables. Consequently, having determined the response surface starting from given random input data, one can immediately determine the statistics of the solution for "new" random input having different statistics, so long as the new data "lives" on the same portion of the probability space as the former. It should be emphasized that such transformation **does not** require that the solution be recomputed using the new random input, as it can be readily determined using spectral projections or alternatively via sampling or collocation. Sampling or collocation approaches are quite suitable for this purpose, since the associated costs are, for most CFD problems of interest, substantially smaller than those required to determine the original stochastic solution (in other words, for large non-linear problems, the cost of uncertainty propagation is much larger than that of sampling the stochastic solution). Thus, it appears to the authors that, an approximate representation of random input data may, in many cases, be efficiently corrected in post-processing stages.

Beyond matters of computational convenience, and of representation of stochastic inputs, it is generally difficult to assess the impact of the basis function representation on the efficiency of the propagation computations. This is the case because, for complex nonlinear problems, generally little is known *a priori* about the statistics of the solution, and the relationship between these statistics and those of the random inputs. On the other hand, if the statistics of the solutions are known or constrained, one may attempt to take advantage of this knowledge by selecting a basis function representation that efficiently captures the known or constrained behavior, appropriately approximating the random inputs using a few elements of this basis, and later correcting for the approximation through post-processing.

An additional complication that has so far received little attention concerns the case where the stochastic solution depends steeply or discontinuously on

the random inputs. In such situations, one would expect that a spectral representation in terms of global basis functions would exhibit severe difficulties. This topic is addressed in the section below, which shows that wavelet-based decompositions may be effective in addressing some of these difficulties.

5.2 *Local Basis Functions*

Uncertainty propagation may be especially challenging in cases where random inputs include critical parameters or bifurcation points. In such situations, the representation of the flow dependence on the uncertain parameters using global polynomial basis may be impractical because of discontinuities or insufficient smoothness along the stochastic dimensions. Specifically, the exponential convergence rate may be lost, and Gibbs phenomena may result in large errors or even global breakdown of the solution. To overcome these drawbacks, local expansions have been proposed in [26, 27]. These expansions use Multi-Wavelets (see [2]) basis consisting in piece-wise continuous multidimensional polynomials.

For zero-order multi-wavelets (MW), one obtains a Wiener-Haar expansion which is a piece-wise constant approximation of the uncertain flow [26], i.e. it provides local averages of the flow over sub-domains of the uncertain parameter space, whose “volumes” are controlled by the resolution level. As the resolution level increases, the flow is averaged over smaller and smaller portions of the parameter space, thus allowing convergence to the exact response surface. In [26] an example is provided for the case of stochastic Rayleigh-Bénard instability in a rectangular domain, the input uncertainty essentially corresponding to a stochastic Rayleigh number which assumes both subcritical and supercritical values. The numerical experiments showed that the (global) Wiener-Legendre expansion was not able to converge to the correct solution, and that the oscillatory character of the polynomials leads to unphysical predictions when the expansion order is increased. On the other hand, the Wiener-Haar computations provide robust estimates which converged towards the exact stochastic solution as the number of refinement levels increased.

The improvement in robustness and stability provided by MW expansions is achieved at the cost of a lower convergence rate, the stochastic errors now being controlled by the polynomial order (p -convergence) and the refinement level (h -convergence). Also the dimension of the spectral basis dramatically increases with the resolution level and polynomial order, especially for problems with a large number of stochastic dimensions n . However, the common situation concerns a smooth dependence of the flow over large portions of the parameter space, where high-order expansions are well suited, separated by localized step/discontinuous variations, where the robustness of low order

expansions highly desired. Thus, an optimal, non-global representation would involve high-order polynomial expansions over large sub-domains of the parameter space, where p -convergence is attractive, and low-order expansions in regions of steep/discontinuous variation, where h -convergence is highly effective. This ideal picture is similar to the spatial spectral-element discretizations strategies, the discretization being now implemented in the space of random data. Since the behavior of the stochastic solution is generally not known *a priori*, an adapted mesh of the parameter space can not be determined before the computations are performed. Thus, automatic refinement strategies are sought in order to tune the local resolution level and the polynomial order. Most of the techniques developed for Automatic Mesh Refinement (AMR) can in principle be applied or adapted for the present purpose. For instance, in [27] an automatic procedure, involving an *a priori* error estimator based on the local MW expansion, was designed to determine the need for local stochastic refinement. Compared to spatial AMR techniques, one observes that refinement of the random parameter space is easier to handle since solutions over sub-domains can be obtained independently. This features substantially simplifies data management, and allows for straightforward parallel implementations.

6 Outlook

As highlighted above, various implementations of PC representations have been recently applied to the development of stochastic NS solvers. These developments have been in large part motivated by the promise of achieving accurate representations of the impact of uncertain input data, at efficiency levels that far exceed those of MC computations. This review has, in particular, identified various areas of recent progress.

The use of PC-based representations for stochastic NS computations is still a developing field. There is, consequently, a large potential for substantial advances. Based on our own recent experiences –and consequently biases– we conclude with a brief outline of some of the corresponding opportunities and challenges:

- (1) The development of flexible and robust computational libraries for accurate and efficient evaluation of PC transformation can be regarded as an essential tool for the construction of stochastic PC-based stochastic codes. Briefly, these libraries have enabled efficient transformation of deterministic codes into stochastic codes. This transformation, however, requires user intervention, primarily to replace deterministic operations with the corresponding functional calls into the stochastic library. An interesting concept worth pursuing consists of an “automating” transformation, in which deterministic operations would be replaced by stochastic counterparts at essentially compilation or during run time. The development of software tools that would enable such key capabilities appears to be present a key opportunity that would benefit and accelerate a wide range of investigations.
- (2) One of the challenges facing PC representations arises in situations in which both the deterministic and stochastic systems exhibit limit cycle oscillations (LCO). To illustrate these challenges, one can consider the idealized case of a linear oscillator having a random, say Gaussian, frequency. The exact solution of such an idealized system, which can be readily determined, indicates that at large time the solution exhibits a random phase that is uniformly distributed over the unit circle. An immediate dilemma facing such situations concerns the selection of a basis, as those based on continuous random variables generally face severe difficulties in providing efficient representations of both the input and the output. Much needed are robust means to overcome such difficulties.
- (3) Another set of challenges concerns situations where one is only interested in assessing the impact of uncertainty on specific observables or components of the solution. These are in many ways akin to the problems just mentioned. For instance, in problems admitting LCOs, one may only be interested in stochastic amplitudes and frequencies, but not in relating

the phase of different stochastic realizations. The development of computational PC methods enabling such “projections” appears to be a worthy endeavor.

- (4) Computational experiences obtained using PC representations in unsteady NS computations have so far been quite encouraging. In particular, efficient schemes have been developed exhibiting superior convergence characteristics. On the other hand, theoretical results concerning the behavior of the systems of stochastic equations resulting from PC representations of stochastic NS equations are lacking. Of particular interest would be the pursuit of rigorous results concerning the stability of such systems of stochastic equations and, if necessary, numerical methods to stabilize the corresponding computations.
- (5) Recent experiences with wavelet-based decompositions in stochastic NS computations have pointed to the potential of constructing highly-efficient, accurate and robust UQ schemes. While experiences gained so far are quite limited, they indicate the promise of local refinement techniques as well as adaptive order methods in which the order of PC expansions is also adapted together with local refinement of random parameter space. These methods are yet to be fully exploited in the context of stochastic NS computations.

Finally, we recall that the development UQ methods for CFD computations has in many cases been motivated by the increasingly-elaborate, underlying physical models, typically including a large number of uncertain parameters. The impact that UQ schemes can bring to such situations is in large part conditioned on a suitable representation of the uncertainty in the model inputs. Though the issue of representation of uncertain inputs has not been central to the present review, it should evidently not be overlooked during implementations. This may represent an especially delicate task in the case of complex models, which may incorporate uncertain, possibly correlated, data gathered from different experiments, observations and/or simulations.

Acknowledgments

The authors acknowledge helpful interactions with collaborators, particularly R. Ghanem, H. Najm, B. Debusschere, and M. Reagan. This work was supported by the Laboratory Directed Research and Development Program at Sandia National Laboratories, by the Defense Advanced Research Projects Agency (DARPA) and Air Force Research Laboratory, Air Force Materiel Command, USAF, under agreement number F30602-00-2-0612. The U.S. government is authorized to reproduce and distribute reprints for Governmental purposes notwithstanding any copyright annotation thereon. Computations were performed at the National Center for Supercomputer Applications. OK also acknowledges support from the Alexander von Humboldt Foundation.

References

- [1] M. Abramowitz and I.A. Stegun. *Handbook of Mathematical Functions*. Dover, 1970.
- [2] B.K. Alpert. A class of bases in L_2 for the sparse representation of integral operators. *SIAM J. Math. Anal.*, 24:246–262, 1993.
- [3] R. Askey and J. Wilson. Some basic hypergeometric polynomials that generalize Jacobi polynomials. *Mem. Amer. Math. Soc.*, 319, 1985.
- [4] R.H. Cameron and W.T. Martin. The orthogonal development of nonlinear functionals in series of Fourier-Hermite functionals. *Ann. Math.*, 48:385–392, 1947.
- [5] C. Canuto, Y. Yousuff Hussaini, A. Quasteroni, and T.A. Zang. *Spectral Methods in Fluid Dynamics*. Springer-Verlag, 1988.
- [6] D. Chenoweth and S. Paolucci. Natural convection in an enclosed vertical layer with large horizontal temperature differences. *J. Fluid Mech.*, 169:173–210, 1986.
- [7] A.J. Chorin. A numerical method for solving incompressible viscous flow problems. *J. Comput. Phys.*, 2:12–26, 1967.
- [8] A.J. Chorin. Gaussian fields and random flow. *Journal of Fluid Mechanics*, 63:21–32, 1974.
- [9] S.C. Crow and G.H. Canavan. Relationship between a Wiener-Hermite expansion and an energy cascade. *Journal of Fluid Mechanics*, 41:387–403, 1970.
- [10] B. Debusschere, H.N. Najm, A. Matta, O.M. Knio, R.G. Ghanem, and O.P. Le Maître. Protein labeling reactions in electrochemical microchannel flow: Numerical prediction and uncertainty propagation. *Physics of Fluids*, 15(8):2238–2250, 2003.
- [11] B.J. Debusschere, H.N. Najm, P.P. Pébray, O.M. Knio, R.G. Ghanem, and O.P. Le Maître. Numerical challenges in the use of Polynomial Chaos representations for stochastic processes. *SIAM J. Sci. Comp.*, 2004. in press.
- [12] R. Ghanem. Ingredients for a general purpose stochastic finite element formulation. *Computer Methods in Applied Mechanics and Engineering*, 168:19–34, 1999.
- [13] R. Ghanem and S. Dham. Stochastic finite element analysis for multiphase flow in heterogeneous porous media. *Transport in Porous Media*, 32:239–262, 1998.
- [14] R.G. Ghanem. Probabilistic characterization of transport in heterogeneous media. *Computer Methods in Applied Mechanics and Engineering*, 158:199–220, 1998.

- [15] R.G. Ghanem and O.M. Knio. A probabilistic framework for the validation and certification of computer simulations. In *Proceedings of 1st JANNAF Modeling and Simulation Subcommittee Meeting*, 2000.
- [16] R.G. Ghanem and R.M. Kruger. Numerical solution of spectral stochastic finite element systems. *Computer Methods in Applied Mechanics and Engineering*, 129:289–303, 1996.
- [17] R.G. Ghanem and P.D. Spanos. A spectral stochastic finite element formulation for reliability analysis. *J. Eng. Mech. ASCE*, 117:2351–2372, 1991.
- [18] R.G. Ghanem and P.D. Spanos. *Stochastic Finite Elements: A Spectral Approach*. Springer Verlag, 1991.
- [19] T.D. Hien and M. Kleiber. Stochastic finite element modeling in linear transient heat transfer. *Computer Methods in Applied Mechanics and Engineering*, 144:111–124, 1997.
- [20] G. Kallianpur. *Stochastic Filtering Theory*. Springer-Verlag, 1980.
- [21] A. Keese and H. G. Matthies. Sparse quadrature as an alternative to Monte Carlo for stochastic finite element techniques. *Proceedings in Applied Mathematics and Mechanics*, 3(1):493–494, 2003.
- [22] J. Kim and P. Moin. Application of a fractional-step method to incompressible navier-stokes equations. *J. Comput. Phys.*, 59:308–323, 1985.
- [23] O.M. Knio and R.G. Ghanem. Polynomial Chaos product and moment formulas : A user utility. Technical report, The Johns Hopkins University, Baltimore, MD, to appear.
- [24] O.P. Le Maître, O.M. Knio, B.D. Debuschere, H.N. Najm, and R.G. Ghanem. A multigrid solver for two-dimensional stochastic diffusion equations. *Computer Methods in Applied Mechanics and Engineering*, 92(41-42):4723–4744, 2003.
- [25] O.P. Le Maître, O.M. Knio, H.N. Najm, and R.G. Ghanem. A stochastic projection method for fluid flow. i. basic formulation. *Journal of Computational Physics*, 173:481–511, 2001.
- [26] O.P. Le Maître, O.M. Knio, H.N. Najm, and R.G. Ghanem. Uncertainty propagation using Wiener-Haar expansions. *Journal of Computational Physics*, 197(1):28–57, 2004.
- [27] O.P. Le Maître, H.N. Najm, R.G. Ghanem, and O.M. Knio. Multi-resolution analysis of Wiener-type uncertainty propagation schemes. *Journal of Computational Physics*, 197(2):502–531, 2004.
- [28] O.P. Le Maître, M.T. Reagan, B. Debuschere, H.N. Najm, R.G. Ghanem, and O.M. Knio. Natural convection in a closed cavity under stochastic, non-Boussinesq conditions. *SIAM J. Sci. Comput.*, 2004. in press.
- [29] O.P. Le Maître, M.T. Reagan, H.N. Najm, R.G. Ghanem, and O.M. Knio. A stochastic projection method for fluid flow. ii. random process. *Journal of Computational Physics*, 181:9–44, 2002.

- [30] J.S. Liu. *Monte Carlo Strategies in Scientific Computing*. Springer Verlag, 2001.
- [31] M. Loève. *Probability Theory*. Springer, 1977.
- [32] A. Majda and J. Sethian. The derivation and numerical solution of the equations for zero-Mach number combustion. *Comb. Sci. and Technology*, 42:185–205, 1985.
- [33] L. Mathelin, M.Y. Hussaini, T.A. Zang, and F. Bataille. Uncertainty propagation for turbulent compressible flow in a quasi-1d nozzle using stochastic methods. *AIAA Journal*, 2004. in press.
- [34] A. Matta. *Numerical Simulation and Uncertainty Quantification in Microfluidic systems*. PhD thesis, Department of Civil Engineering, Johns Hopkins University, 2003.
- [35] H. Matthies and A. Keese. Galerkins methods for linear and nonlinear elliptic stochastic partial differential equations. Report 2003-08, Inst. Scientific Computing, Technical University Braunschweig, Technical University Braunschweig Brunswick, Germany, 2003.
- [36] H.G. Matthies, C.E. Brenner, C.G. Bucher, and C.G. Soares. Uncertainties in probabilistic numerical analysis of structures and solids - stochastic finite-elements. *Structural Safety*, 19(3):283–336, 1997.
- [37] M. McKay, R. Beckman, and W. Conover. A comparison of three methods for selecting values of input variables in the analysis of output from a computer code. *Technometrics*, 21(2):239–245, 1979.
- [38] W.C. Meecham and D.T. Jeng. Use of the Wiener-Hermite expansion for nearly normal turbulence. *Journal of Fluid Mechanics*, 32:225, 1968.
- [39] H.N. Najm, M.T. Reagan, O.M. Knio, R.G. Ghanem, and O.P. Le Maître. Uncertainty quantification on reacting flow modelling. Technical Report 2003-8598, SANDIA, 2003.
- [40] E. Novak and K. Ritter. High-dimensional integration of smooth functions over cubes. *Numerische Mathematik*, 75:79–97, 1996.
- [41] E. Novak and K. Ritter. The curse of dimension and a universal method for numerical integration. In G. Nürnberger, J. W. Schmidt, and G. Walz, editors, *Multivariate Approximation and Splines, ISNM*, pages 177–188. Birkhäuser, Basel, 1997.
- [42] E. Novak and K. Ritter. Simple cubature formulas with high polynomial exactness. *Constructive Approximation*, 15:499–522, 1999.
- [43] K. Petras. Fast calculation of coefficients in the Smolyak algorithm. *Numerical Algorithms*, 26:93–109, 2001.
- [44] B.D. Phenix, J.L. Dinero, M.A. Tatang, J.W. Tester, J.B. Howard, and G.J. McRae. Incorporation of Parametric Uncertainty into Complex Kinetic Mechanisms: Application to Hydrogen Oxidation in Supercritical Water. *Combustion and Flame*, 112:132–146, 1998.

- [45] P. Le Quéré, R. Masson, and P. Perron. A Chebychev collocation algorithm for 2d non-Boussinesq convection. *J. Comput. Phys.*, 103:320–334, 1992.
- [46] S.A. Smolyak. Quadrature and interpolation formulas for tensor products of certain classes of functions. *Dokl. Akad. Nauk SSSR*, 4:240–243, 1963.
- [47] S. Wiener. The Homogeneous Chaos. *Amer. J. Math.*, 60:897–936, 1938.
- [48] D.B. Xiu and G.E. Karniadakis. The Wiener-Askey Polynomial Chaos for stochastic differential equations. *SIAM J. Sci. Comput.*, 24:619–644, 2002.
- [49] D.B. Xiu and G.E. Karniadakis. Modeling uncertainty in flow simulations via generalized Polynomial Chaos. *Journal of Computational Physics*, 187:137–167, 2003.